RSC Advances

PAPER

View Article Online
View Journal | View Issue

Check for updates

Cite this: *RSC Adv.*, 2020, **10**, 29705

Searching for double σ- and π-aromaticity in borazine derivatives†

Ricardo Pino-Rios,[a] Alejandro Vásquez-Espinal,[b] Osvaldo Yañez[bc] and William Tiznado[b]

Received 29th April 2020
Accepted 31st July 2020

DOI: 10.1039/d0ra05939k

rsc.li/rsc-advances

Inspired by the double-aromatic (σ and π) $C_6H_3^+$, $C_6I_6^{2+}$, and $C_6(SePh)_6^{2+}$ ring-shaped compounds, herein we theoretically study their borazine derivative analogues. The systems studied are the cation and dications with formulas $B_3N_3H_3^+$, $B_3N_3Br_6^{2+}$, $B_3N_3I_6^{2+}$, $B_3N_3(SeH)_6^{2+}$, and $B_3N_3(TeH)_6^{2+}$. Our DFT calculations indicate that the ring-shaped planar structures of $B_3N_3H_3^+$, $B_3N_3I_6^{2+}$, and $B_3N_3(TeH)_6^{2+}$ are more stable in the singlet state, while those of $B_3N_3Br_6^{2+}$ and $B_3N_3(SeH)_6^{2+}$ prefer the triplet state. Besides, exploration of the potential energy surface shows that the ring-shaped structure is the putative global minimum only for $B_3N_3I_6^{2+}$. According to chemical bonding analysis, $B_3N_3H_3^+$, $B_3N_3I_6^{2+}$, and $B_3N_3(TeH)_6^{2+}$ have σ and π delocalized bonds. The number of delocalized σ/π electrons is 2/6 for the first, and 10/6 for the second and third, similar to what their carbon analogs exhibit. Finally, the analysis of the magnetically induced current density allows $B_3N_3H_3^+$, $B_3N_3I_6^{2+}$, and $B_3N_3(TeH)_6^{2+}$ to be classified as strongly σ aromatic, and poorly π aromatic compounds.

Introduction

In 1979, Schleyer and co-workers introduced the concept of double aromaticity. They showed that the 3,5-dehydrophenyl cation (**1**, Scheme 1) exhibits two orthogonal Hückel frameworks, consisting of 6π and 2σ electrons.[1] Since then, many compounds exhibiting double aromaticity have been predicted theoretically,[2–11] with some even being experimentally characterized.[12–17] For instance, in 1988, Martin and Sagl[15] reported the synthesis of the hexaiodobenzene dication, $C_6I_6^{2+}$ (**2**, Scheme 1), a double-aromatic compound with two concentric delocalization circuits, consisting of 6π electrons delocalized around the C_6 ring, and 10σ electrons delocalized around the I_6 ring. This finding paved the way to synthesize and characterize, by X-ray diffraction, the first double-aromatic "bench-stable" molecule, the hexakis(phenylselenyl)benzene dication[16] (**3**, Scheme 1).

Here we evaluate the structure, stability, chemical bonding, and magnetic response properties of $B_3N_3H_3^+$, $B_3N_3Br_6^{2+}$, $B_3N_3I_6^{2+}$, $B_3N_3(SeH)_6^{2+}$ and $B_3N_3(TeH)_6^{2+}$ (**4**, **5**, **6**, **7** and **8**, Scheme 1) systems in pursuit of expanding the family of double-aromatic compounds.

As we can see in Scheme 1, compounds **4–8** are analogues to the double-aromatic benzene derivatives referred above (**1**, **2** and **3**, Scheme 1), where C_6 is replaced by the B_3N_3 ring. It is important to note that the aromatic character of borazine has been a much-debated topic in the past with contrasting conclusions.[18–27] There is even disagreement among studies based on the same criteria, *i.e.* magnetic. For instance, various studies have evaluated current density maps, both global and

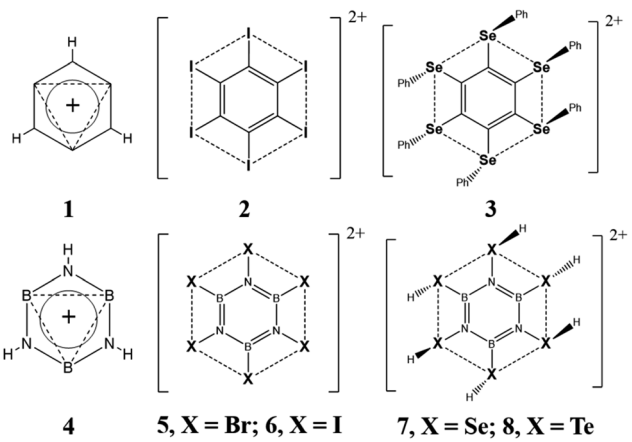

Scheme 1 Structures of double-aromatic benzene derivatives (**1–3**) and their borazine derivative analogues. Dashed lines represent the σ delocalization circuits.

[a]*Laboratorio de Química Teórica, Facultad de Química y Biología, Universidad de Santiago de Chile (USACH), Av. Libertador Bernardo O'Higgins 3363, Santiago, Estación Central, Región Metropolitana, Chile. E-mail: ricardo.pino@usach.cl*

[b]*Computational and Theoretical Chemistry Group, Departamento de Ciencias Químicas, Facultad de Ciencias Exactas, Universidad Andres Bello, República 498, Santiago, Chile. E-mail: wtiznado@unab.cl*

[c]*Center for Bioinformatics and Integrative Biology (CBIB), Facultad de Ciencias de la Vida, Universidad Andres Bello, Av. Republica 330, Santiago 8370146, Chile*

† Electronic supplementary information (ESI) available. See DOI: 10.1039/d0ra05939k

Open Access Article. Published on 11 August 2020. Downloaded on 12/8/2025 10:52:22 PM.
This article is licensed under a Creative Commons Attribution-NonCommercial 3.0 Unported Licence.

Open Access Article. Published on 11 August 2020. Downloaded on 12/8/2025 10:52:22 PM.
This article is licensed under a Creative Commons Attribution-NonCommercial 3.0 Unported Licence.

dissected (σ and π), and concluded that borazine does not support a net diatropic current (aromaticity indicator) around the B_3N_3 ring. Instead, it displays three local π delocalization pathways (around the N atoms).[18–20] Given the large difference in electronegativity between the two participating elements, $\Delta\chi$(N,C) = 1.0,[28] it sounds reasonable that the π electrons are more polarized to the N atoms. However, analysis of both the induced magnetic field[26,27] and the intensity of the ring current strengths (RCS)[23,24,26] suggests that borazine does sustain a net diatropic ring current (less intense than that of benzene). Given these discrepancies, why would we assume that the compounds **4–8**, in this work, would have a double aromatic character? Our answer is based on the quantitative analyses on the aromaticity of borazine available in the literature. The most modern analyses, based on the energetic criteria (aromatic stabilization energy, ASE), agree that the aromaticity of borazine is at least 20% benzene's.[21,22,26] For instance, Baranac-Stojanović *et al.* reported extra cyclic resonance energy (ECRE) values, at B3LYP/6-311+G(d,p) level, of 89.35 and 20.18 kcal mol^{-1} for benzene and borazine, respectively.[22] Furthermore, in 2013, our group estimated that the aromaticity of borazine is about 30% benzene's, according to the energetic and magnetic criteria.[26] The first one, using isodesmic reactions to estimate ASEs, and the second one, through the analysis of three properties: the induced magnetic field, the nucleus independent chemical shift (NICS) and the RCS. These results contrast slightly with RCSs of benzene and borazine (12.8 and 2.1 nA T^{-1}), calculated at RHF level, by Monaco *et al.*[29] However, they agree with both RCS values for benzene and borazine reported most recently by Monaco *et al.* (11.8 and 3.0 nA T^{-1})[23] and with our current calculations (11.8 and 3.6 nA T^{-1}). Under this energetic and magnetic evidences, we consider that the B_3N_3 ring, of the systems studied here, should sustain at least a slight π-aromatic character. The latter, together with the fact that the chemistry of borazine, and its derivatives, is well established,[30–32] supports our proposal of compounds **4–8**, as potential aromatic derivatives of borazine.

Computational details

In order to evaluate the stability, chemical bonding and aromatic character of the proposed systems, we used the following methodologies:

(a) The potential energy surface (PES) of systems, **4**, **6** and **8**, was explored *via* the AUTOMATON program.[33] This program uses a probabilistic automaton method to generate an initial population that evolves to the best individual (global minimum, GM) through genetic operations. The searches were performed *via* the PBE0 [34] functional in conjunction with the SDDALL[35,36] basis. The low-lying structures were subsequently re-minimized at the PBE0-D3 [37]/def2-TZVP[38] level. We used an initial population of 5*X* (*X* = number of atoms of the system), this small population showed to be enough to successfully identify the lowest energy structures of many clusters and molecules.[39–43] Additionally, we evaluated the dynamic behavior of compounds **4**, **6** and **8** (for an insight into their kinetic stability), employing Born–Oppenheimer molecular dynamic (BOMD) simulations.[44] Geometry optimizations, vibrational frequency and BOMD calculations were carried out using the Gaussian 16 program.[45]

(b) Chemical bonding was analyzed through the adaptive natural density partitioning (AdNDP) method,[46,47] which is an extension of the natural bond orbital (NBO) analysis.[48–50] AdNDP allows for electronic density partitioning of a molecular system in terms of *n*-center two-electron (*n*c-2e) bonds, with *n* ranging from one to the total number of atoms in the molecule. Thus, AdNDP recovers the Lewis elements (lone pairs, and 2c-2e bonds), as well as the delocalized *n*c-2e bonds. Therefore, the number of *n*c-2e ($n > 2$) delocalized bonds allows to classify a system as aromatic (4N + 2) or anti-aromatic (4N), following Hückel's rule.[51–53]

(c) The aromatic character was also assessed through the magnetic criteria. Current density maps, induced by an external magnetic field, were calculated for this purpose. These maps allowed us to easily observe the diatropicity/paratropicity of the examined systems, and to correlate these magnetic patterns with their aromatic/antiaromatic character.[54–56] Additionally, the ring current flow was integrated to estimate the ring current strength (RCS) and to use it as a quantitative criterion for aromaticity.[57–59] In general, a positive and a negative RCS value indicate an aromatic and an anti-aromatic character, respectively. Similarly, the larger the absolute value of the RCS, the higher the (anti) aromatic character of the studied molecule. However, it is more difficult to establish an exact RCS value for nonaromatic systems. The value must be close to zero, but how close? To answer this, we need to compare them with suitable references. In this paper, we have calculated the RCSs of a series of five-member C_4XH_4 rings, for which Mo and Schleyer reported their "extra cyclic resonance energy" (ECRE) to characterize and measure the extra stabilization (aromaticity).[60] ECRE was computed using block-localized wave function (BLW) method[61] and adequate isodesmic reactions. The simple linear correlation of the RCSs *vs.* ECREs is excellent ($r^2 = 0.97$). Furthermore, using the linear equation of this correlation, a value of 0 kcal mol^{-1} ECRS (nonaromatic) would correspond to an RCS value of 0.88 nA T^{-1} (see Table S1 and Scheme S1 in the ESI†). This analysis allows us to consider RCS values higher than 1.5 nA T^{-1} here, as indicative of aromatic character. In addition, our group has shown that RCS correlates very well with NICS, when the latter are measured properly.[62–65]

Results and discussion

We began by analyzing compound **4**, which is not the global minimum on the $B_3N_3H_3^+$ PES, but it lies at 49.3 kcal mol^{-1} above the lowest singlet state energy structure at PBE0 [34]-D3 [37]/def2TZVP level.[38] However, **4** is a true minimum on its PES since all its vibrational frequencies are positive. The 22 lowest singlet state energy structures of $B_3N_3H_3^+$, identified by the AUTOMATON program, are reported in Fig. S1.† It is important to note that AUTOMATON did not identify structure **4**, since this program focuses on identifying the GM structure. However, AUTOMATON allowed discarding **4** as the putative GM.

Interestingly, the structure of **4** is similar to that of its analog **1**. As with the carbon angles bearing no hydrogens at **1**, the

 This journal is © The Royal Society of Chemistry 2020

Open Access Article. Published on 11 August 2020. Downloaded on 12/8/2025 10:52:22 PM.
This article is licensed under a Creative Commons Attribution-NonCommercial 3.0 Unported Licence.

angle widens in the boron of compound **4**. The optimized structure at PBE0-D3/def2TZVP level shows angles NBN to be 167°. The B–B Wiberg bond index (WBI)[66,67] (0.45|*e*| at PBE0-D3/def2TZVP level) is similar, to that obtained for the dehydrogenated carbon atoms in **1**, which according to Schleyer, has a σ 3c-2e delocalized bond. This result supports a possible in-plane 3c-2e σ-bonding interaction involving the B_3 ring.

According to the AdNDP results reported in Fig. 1, the 26 valence electrons (13 pairs) are distributed in 6 classical B–N σ-bonds (2c-2e) and 3 classical N–H σ-bonds. All other bonds are delocalized. There are three 6c-2e π-bonds (involving the B_3N_3 ring), and one 3c-2e σ-bond (involving the B_3 ring). These results agree with the WBI predictions. Note that 6π/2σ electron counting all conform to the (4*n* + 2) Hückel rule, providing further support for the double-aromatic character of **4**. Interestingly, AdNDP predicts that chemical bonding in compound **4** is similar to that in **1**, the 3,5 dehydrophenyl cation ($C_6H_3^+$; Fig. 1b).

Fig. 2 depicts the magnetically induced current densities calculated in planes located at 1 a_0 (1 bohr) above the molecular plane of **4** (**1** is also included for comparison). The ring current strength (RCS) was computed by integrating the ring current flux that passes along interatomic surfaces defined by the quantum theory of atoms in molecules (QTAIM).[58,59] Diatropic currents are assumed to circle clockwise, and the paratropic ones to circle anticlockwise. The current density map of **4** exhibits two diatropic ring currents (one σ and one π) distributed around the molecular ring (Fig. 2a and b). As expected, compound **1** also exhibits diatropic σ and π ring currents (Fig. 2c and d) with a σ-current flow distribution pattern similar to **4**. However, π ring current flow patterns are different for **1** and **4**: the ring current is continuous and clearly noticeable at **1**, but at **4**, there are two types of current, the diatropic local one on each nitrogen atom, and the ring current. Since the local is stronger than the ring current, the pattern for **4** does not exhibit the same continuity as in **1**. How intense are these current flows, and therefore, how aromatic is system **4**? The σ-RCS/π-RCS value of 5.4/1.5 nA T^{-1} predicts system **4** to be a σ-aromatic/poorly π-aromatic compound; whereas σ-RCS/π-RCS value of 11.1/9.9 nA T^{-1} predicts system **1** to be a σ-aromatic/π-aromatic compound. This assignment is made on the basis of the reference σ-RCS/π-RCS values of 0.5/11.7 nA T^{-1} for benzene, which is a σ-nonaromatic/strongly π-aromatic system. It is important to note that **1** is the global minimum structure for the $C_6H_3^+$ combination (at the CCSD(T)-F12b/cc-pVTZ + ZPE(B3LYP/cc-pVTZ)//CCSD(T)/cc-pVTZ level).[68] Thus, in the light of our current density analysis, it is possible to suggest that the high σ and π aromatic character must be contributing to ring shaped stabilization of $C_6H_3^+$. Whereas system 4, despite its substantial σ-diatropic character, is not an energetically competitive isomer.

We now focus on discussing our results for the set of per-substituted borazine dications, $B_3N_3Br_6^{2+}$ (**5**), $B_3N_3I_6^{2+}$ (**6**), $B_3N_3(SeH)_6^{2+}$ (**7**) and $B_3N_3(TeH)_6^{2+}$ (**8**). From this series, only structures **6** and **8** are more stable in the singlet state, while structures **5** and **7** prefer the triplet state (at PBE0-D3/def2TZVP

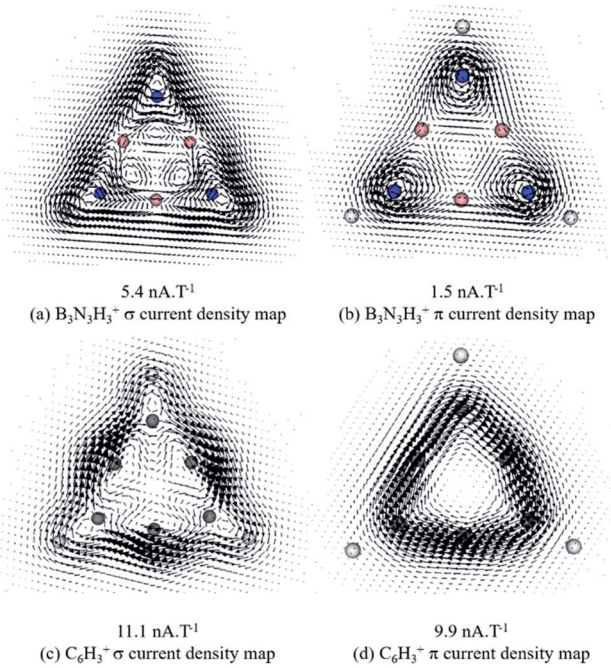

Fig. 2 Vector maps of dissected magnetically induced current density (MICD) at 1 a_0 above the molecular plane of (**4**) $B_3N_3H_3^+$ (top) and (**1**) $C_6H_3^+$ (bottom).

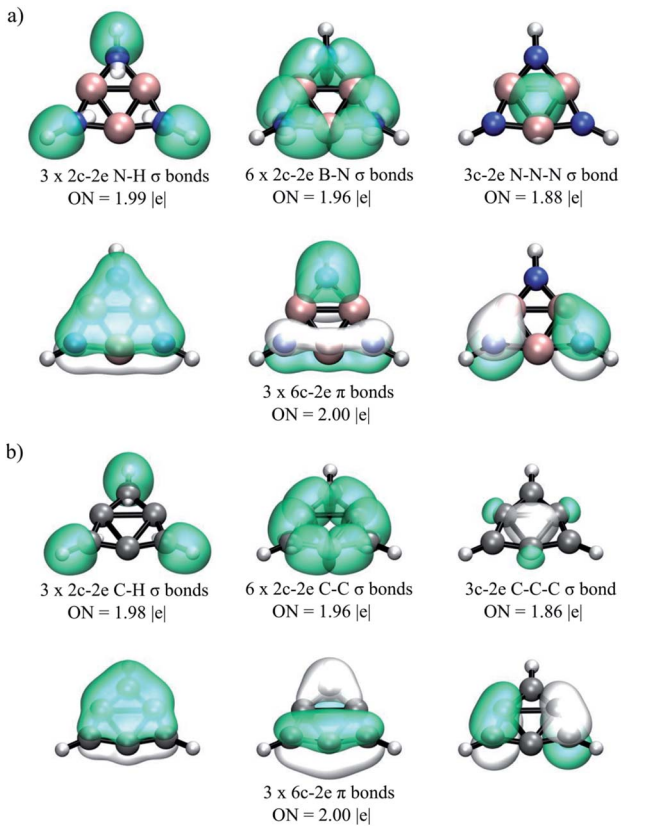

Fig. 1 AdNDP bonding pattern of (a) $B_3N_3H_3^+$ (**4**) as compared to that of (b) $C_6H_3^+$ (**1**). Occupation numbers (ONs) are shown.

Open Access Article. Published on 11 August 2020. Downloaded on 12/8/2025 10:52:22 PM.
This article is licensed under a Creative Commons Attribution-NonCommercial 3.0 Unported Licence.

level). Therefore, **5** and **7** are discarded as suitable candidates for double-aromatic systems.

After exploring its PES, AUTOMATON predicts **6** as the lowest energy structure for the $B_3N_3I_6^{2+}$ combination, whereas **8** lies 68.7 kcal mol^{-1} above the lowest energy singlet-state structure for $B_3N_3(TeH)_6^{2+}$ combination (all structures identified by AUTOMATON within 70 kcal mol^{-1} above the global minimum for $B_3N_3(TeH)_6^{2+}$ are reported in Fig. S2†). It is important to note that canonical AUTOMATON procedure provided dissociated structures as the lowest energy isomers for these systems. Thus, we performed a guided search, which consists in replacing the H by I or by the Te–H fragment in the 60 lowest energy structures identified by AUTOMATON for borazine, subsequently the resulting structures were used as initial population in the AUTOMATON's PES exploration of $B_3N_3I_6^{2+}$ and $B_3N_3(TeH)_6^{2+}$. The second isomer of $B_3N_3I_6^{2+}$ is the triplet-state ring shaped C_{2v} structure and lies 2.0 kcal mol^{-1} above **6**. Singlet and triplet isomers under 30 kcal mol^{-1} identified by AUTOMATON for $B_3N_3I_6^{2+}$ combination are reported in Fig. S3 and S4 in the ESI,† respectively.

At the optimized structures (at PBE0-D3/def2TZVP level) of **6** and **8**, the B–N distances are 1.42 and 1.43 Å respectively, whereas I–I, and Te–Te distances are 3.49 and 3.55 Å, respectively. The WBI value for B–N in compound **6** and **8** are 0.94, very similar to the B–N WBI value in borazine, 1.02, suggesting that B_3N_3 ring in compound **6** and **8** is bonded in a similar way to the B_3N_3 ring of the borazine. On the other hand, WBI values for I–I and Te–Te bonds are both 0.13, suggesting a covalent bonding interaction between these atoms.

According to AdNDP, the bonding pattern of **6** is composed of localized and delocalized elements (Fig. 3a). The localized part is found as twelve lone pairs in the I atoms (two LPs on each one), six classical B–N 2c-2e σ-bonds, three 2c-2e B–I σ-bonds, and three 2c-2e N–I σ-bonds. The delocalized elements are found as three 6c-2e π-bonds (around the B_3N_3 ring), and five 6c-2e σ-bonds (around the I_6 ring). Thus, AdNDP analysis classifies **6** as a 6π/10σ electron system, doubly satisfying the $(4n + 2)$ Hückel's rule, providing further support for its double-aromatic character. Note that AdNDP predicts that chemical bonding in compound **6** is similar to that in **2** ($C_6I_6^{2+}$; Fig. 3b). Moreover, under the same analysis scheme, system **8** shows a very similar chemical bonding pattern to the one shown for system **6**, as can be seen in Fig. S5 in the ESI.†

Fig. 4 depicts the magnetically induced current densities calculated in planes located at 1 a_0 (1 bohr) above the molecular plane of **6** (**2** is also included for comparison). The ring current strength (RCS) was computed by integrating the ring current flux that passes along C–C, B–N and I–I interatomic surfaces, defined by the quantum theory of atoms in molecules (QTAIM). The current density maps of **6** exhibit two diatropic ring currents, one *outer*-σ (*o*-σ) and intense distributed around I_6 ring, and the other *inner*-π (*i*-π) and weak distributed around B_3N_3 ring (Fig. 4a and b). Compound **2** exhibits a similar *o*-σ-ring current flow pattern to **6** but a different *i*-π ring current flow pattern, which is strong in **2**. Moreover, the *o*-σ-RCS/*i*-π-RCS value of 14.3/3.4 nA T^{-1} predicts system **6** to be a σ-aromatic/poorly π-aromatic compound, whereas *o*-σ-RCS/*i*-π-RCS value of 14.9/10.5 nA T^{-1} predicts system **2** as a σ-aromatic/π-aromatic compound. For compound **8**, a similar pattern to **6** is found, with *o*-σ-RCS/*i*-π-RCS value of 8.5/3.6 nA T^{-1} (see Fig. S6 in the ESI†). Thus, according to ring currents, the borazine derivatives **6** and **8** are σ-aromatic and weakly π-aromatic systems.

Finally, BOMD simulations were performed to evaluate the dynamic behavior of compounds **4**, **6** and **8** (Movies S1, S2 and

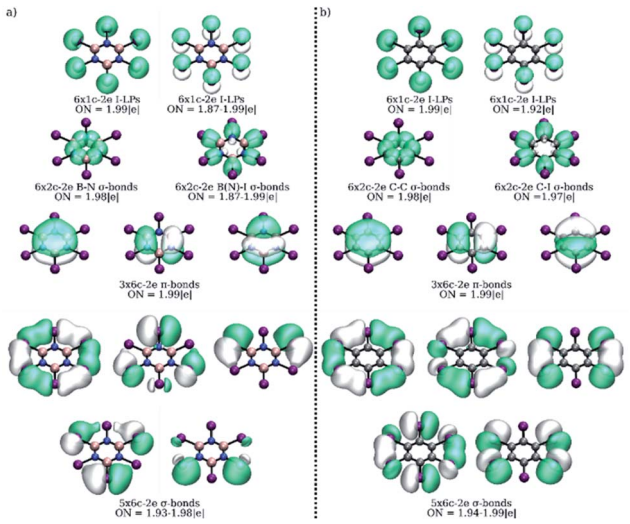

Fig. 3 AdNDP bonding pattern of (a) $B_3N_3I_6^{2+}$ (**6**) as compared to that of (b) $C_6I_6^{2+}$ (**2**). Occupation numbers (ONs) are shown.

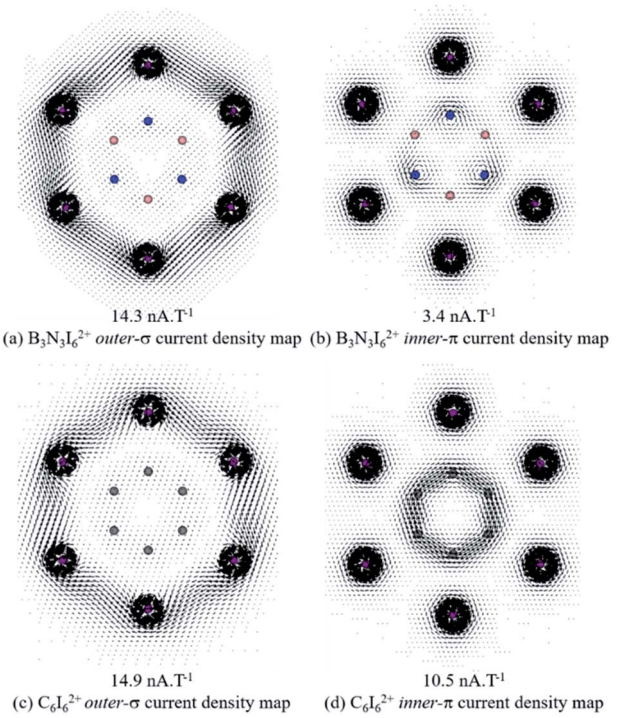

Fig. 4 Vector maps of dissected magnetically induced current density (MICD) at 1 a_0 above the molecular plane of $B_3N_3I_6^{2+}$ (top) and $C_6I_6^{2+}$ (bottom).

 This journal is © The Royal Society of Chemistry 2020

Open Access Article. Published on 11 August 2020. Downloaded on 12/8/2025 10:52:22 PM.
This article is licensed under a Creative Commons Attribution-NonCommercial 3.0 Unported Licence.

S3 in ESI†). The corresponding movies are available in the ESI.† We found that a cyclic arrangement persists over the period of time considered for the dynamics (30 ps), at 900 K. Interestingly, the GM for the combination $B_3N_3(TeH)_6^{2+}$ is not kinetically stable, dissociating in the first steps of the BOMD at 900 K (see Movie S4 in the ESI†). These results suggest good kinetic stability for these compounds, which in conjunction with the evidence that **6** is the putative global minimum for the $B_3N_3I_6^{2+}$ combination, hold promise for its experimental realization.

Conclusions

In summary, we examined five double σ and π aromatic candidates with ring-shaped structures, $B_3N_3H_3^+$ (**4**), $B_3N_3Br_6^{2+}$(**5**), $B_3N_3I_6^{2+}$(**6**), $B_3N_3(SeH)_6^{2+}$ (**7**) and $B_3N_3(TeH)_6^{2+}$ (**8**), derived by isoelectronic substitution of the C_6 ring of the parent species, $C_6H_3^+$, $C_6Br_6^{2+}$, $C_6I_6^{2+}$ $C_6(SeH)_6^{2+}$, and $C_6(TeH)_6^{2+}$. From this series, only **4**, **6**, and **8** structures are more stable in singlet state, whereas **5** and **7** prefer the triplet state. However, the energy of **4** and **8** is 63.2 kcal mol^{-1} and 68.7 kcal mol^{-1} higher than that of the corresponding lowest energy singlet state structure respectively, but structure **6** is the putative global minima on its PES. Moreover, the *ab initio* BOMD simulations revealed that **6** and **8** structures are rather rigid, persisting over the period of time considered for the dynamics (30 ps), at 900 K. Hence, these results suggest that it might be possible to detect **6** as the thermodynamically and kinetically viable structures in the gas phase. Another promising approach would be to replace TeH by TeR ligands, to include steric protection by using bulky *R*-groups, considering that **8** shows reasonable kinetic stability (according to the BOMD simulations).

Conflicts of interest

There are no conflicts to declare.

Acknowledgements

The authors are grateful for the financial support of the Fondecyt Grant No. 1181165 and Fondecyt postdoctorado No. 3180119. Powered@NLHPC: this research was partially supported by the supercomputing infrastructure of the NLHPC (ECM-02).

References

1 J. Chandrasekhar, E. D. Jemmis and P. v. R. Schleyer, Double aromaticity: aromaticity in orthogonal planes. The 3,5-dehydrophenyl cation, *Tetrahedron Lett.*, 1979, **20**, 3707–3710.

2 P. v. R. Schleyer, H. Jiao, M. N. Glukhovtsev, J. Chandrasekhar and E. Kraka, Double aromaticity in the 3,5-dehydrophenyl cation and in cyclo[6] carbon, *J. Am. Chem. Soc.*, 1994, **116**, 10129–10134.

3 S. Martín-Santamaría and H. S. Rzepa, Double aromaticity and anti-aromaticity in small carbon rings, *Chem. Commun.*, 2000, 1503–1504.

4 M. Hofmann and A. Berndt, (π + σ)-double aromatic and π,σ-mixed aromatic boron compounds with two electrons delocalized over three centers, *Heteroat. Chem.*, 2006, **17**, 224–237.

5 M. D. Wodrich, C. Corminboeuf, S. S. Park and P. v. R. Schleyer, Double aromaticity in monocyclic carbon, boron, and borocarbon rings based on magnetic criteria, *Chem.–Eur. J.*, 2007, **13**, 4582–4593.

6 D. Y. Zubarev, B. B. Averkiev, H.-J. Zhai, L.-S. Wang and A. I. Boldyrev, Aromaticity and antiaromaticity in transition-metal systems, *Phys. Chem. Chem. Phys.*, 2008, **10**, 257–267.

7 P. W. Fowler, N. Mizoguchi, D. E. Bean and R. W. A. Havenith, Double Aromaticity and Ring Currents in All-Carbon Rings, *Chem.–Eur. J.*, 2009, **15**, 6964–6972.

8 C. Romanescu, T. R. Galeev, W. Li, A. I. Boldyrev and L. S. Wang, Aromatic Metal-Centered Monocyclic Boron Rings: Co©B8- and Ru©B9-, *Angew. Chem., Int. Ed.*, 2011, **50**, 9334–9337.

9 F. Feixas, E. Matito, J. Poater and M. Solà, Metalloaromaticity, *Wiley Interdiscip. Rev.: Comput. Mol. Sci.*, 2013, **3**, 105–122.

10 C. Romanescu, T. R. Galeev, W.-L. Li, A. I. Boldyrev and L.-S. Wang, Transition-metal-centered monocyclic boron wheel clusters ($M©B_n$): a new class of aromatic borometallic compounds, *Acc. Chem. Res.*, 2013, **46**, 350–358.

11 T. Ou, W. J. Tian, X. R. You, Y. J. Wang, K. Wang and H. J. Zhai, On the structure and bonding in the $B_4O_4^+$ cluster: a boron oxide analogue of the 3,5-dehydrophenyl cation with π and σ double aromaticity, *Phys. Chem. Chem. Phys.*, 2015, **17**, 29697–29706.

12 H.-J. Zhai, B. Kiran, J. Li and L.-S. Wang, Hydrocarbon analogues of boron clusters—planarity, aromaticity and antiaromaticity, *Nat. Mater.*, 2003, **2**, 827–833.

13 A. N. Alexandrova, H.-J. Zhai, L.-S. Wang and A. I. Boldyrev, Molecular Wheel B_8^{2-} as a New Inorganic Ligand. Photoelectron Spectroscopy and ab Initio Characterization of LiB_8^-, *Inorg. Chem.*, 2004, **43**, 3552–3554.

14 A. Van Orden and R. J. Saykally, Small carbon clusters: spectroscopy, structure, and energetics, *Chem. Rev.*, 1998, **98**, 2313–2358.

15 D. J. Sagl and J. C. Martin, The stable singlet ground state dication of hexaiodobenzene: possibly a sigma-delocalized dication, *J. Am. Chem. Soc.*, 1988, **110**, 5827–5833.

16 S. Furukawa, M. Fujita, Y. Kanatomi, M. Minoura, M. Hatanaka, K. Morokuma, K. Ishimura and M. Saito, Double aromaticity arising from σ- and π-rings, *Commun. Chem.*, 2018, **1**, 1–7.

17 A. I. Boldyrev and L.-S. Wang, All-Metal Aromaticity and Antiaromaticity, *Chem. Rev.*, 2005, **105**, 3716–3757.

18 A. Soncini, P. W. Fowler and L. W. Jenneskens, in *Intermolecular Forces and Clusters I*, Springer, 2005, pp. 57–79.

19 E. Steiner, P. W. Fowler and R. W. A. Havenith, Current Densities of Localized and Delocalized Electrons in Molecules, *J. Phys. Chem. A*, 2002, **106**, 7048–7056.

Open Access Article. Published on 11 August 2020. Downloaded on 12/8/2025 10:52:22 PM.
This article is licensed under a Creative Commons Attribution-NonCommercial 3.0 Unported Licence.

20 A. Soncini and P. W. Fowler, Ipsocentric and allocentric methods of mapping induced current density, *Chem. Phys. Lett.*, 2004, **396**, 174–181.
21 I. Fernandez and G. Frenking, Direct estimate of conjugation and aromaticity in cyclic compounds with the EDA method, *Faraday Discuss.*, 2007, **135**, 403–421.
22 M. Baranac-Stojanović and M. Stojanović, Substituent effects on cyclic electron delocalization in symmetric B- and N-trisubstituted borazine derivatives, *RSC Adv.*, 2013, **3**, 24108–24117.
23 G. Monaco and R. Zanasi, The making of ring currents, *Phys. Chem. Chem. Phys.*, 2016, **18**, 11800–11812.
24 G. Monaco, R. Zanasi, S. Pelloni and P. Lazzeretti, Relative weights of σ and π ring currents in a few simple monocycles, *J. Chem. Theory Comput.*, 2010, **6**, 3343–3351.
25 R. Carion, V. Liégeois, B. Champagne, D. Bonifazi, S. Pelloni and P. Lazzeretti, On the Aromatic Character of 1,2-Dihydro-1,2-azaborine According to Magnetic Criteria, *J. Phys. Chem. Lett.*, 2010, **1**, 1563–1568.
26 J. J. Torres-Vega, A. Vásquez-Espinal, J. Caballero, M. L. Valenzuela, L. Alvarez-Thon, E. Osorio and W. Tiznado, Minimizing the Risk of Reporting False Aromaticity and Antiaromaticity in Inorganic Heterocycles Following Magnetic Criteria, *Inorg. Chem.*, 2014, **53**, 3579–3585.
27 R. Islas, E. Chamorro, J. Robles, T. Heine, J. C. Santos and G. Merino, Borazine: to be or not to be aromatic, *Struct. Chem.*, 2007, **18**, 833–839.
28 L. Pauling, *The Nature of the Chemical Bond*, Cornell University Press, Ithaca, NY, 1960, vol. 260.
29 M. R. Hoare and P. Pal, Physical cluster mechanics: Statics and energy surfaces for monatomic systems, *Adv. Phys.*, 1971, **20**, 161–196.
30 A. Stock and E. Pohland, Borwasserstoffe, IX.: B3N3H6, *Ber. Dtsch. Chem. Ges. A*, 1926, **59**, 2215–2223.
31 T. Wideman and L. G. Sneddon, Convenient procedures for the laboratory preparation of borazine, *Inorg. Chem.*, 1995, **34**, 1002–1003.
32 A. H. Cowley, H. H. Sisler and G. E. Ryschkewitsch, THE CHEMISTRY OF BORAZINE. III. B-SILYL BORAZINES, *J. Am. Chem. Soc.*, 1960, **82**, 501–502.
33 O. Yañez, R. Báez-Grez, D. Inostroza, W. A. Rabanal-León, R. Pino-Rios, J. Garza and W. Tiznado, AUTOMATON: a program that combines a probabilistic cellular automata and a genetic algorithm for global minimum search of clusters and molecules, *J. Chem. Theory Comput.*, 2019, **15**, 1463–1475.
34 C. Adamo and V. Barone, Toward Reliable Density Functional Methods Without Ajustable Parameters: The PBE0 Model, *J. Chem. Phys.*, 1999, **110**, 6158.
35 A. Bergner, M. Dolg, W. Kuchle, H. Stoll and H. Preuss, Ab-Initio Energy-Adjusted Pseudopotentials for Elements of Groups 13–17, *Mol. Phys.*, 1993, **80**, 1431–1441.
36 G. Igel-Mann, H. Stoll and H. Preuss, Pseudopotentials for main group elements (IIIa through VIIa), *Mol. Phys.*, 1988, **65**, 1321–1328.
37 S. Grimme, J. Antony, S. Ehrlich and H. Krieg, A consistent and accurate ab initio parametrization of density functional dispersion correction (DFT-D) for the 94 elements H–Pu, *J. Chem. Phys.*, 2010, **132**, 154104.
38 F. Weigend and R. Ahlrichs, Balanced basis sets of split valence, triple zeta valence and quadruple zeta valence quality for H to Rn: design and assessment of accuracy, *Phys. Chem. Chem. Phys.*, 2005, **7**, 3297–3305.
39 O. Yañez, A. Vásquez-Espinal, R. Báez-Grez, W. A. Rabanal-León, E. Osorio, L. Ruiz and W. Tiznado, Carbon rings decorated with group 14 elements: new aromatic clusters containing planar tetracoordinate carbon, *New J. Chem.*, 2019, **43**, 6781–6785.
40 O. Yañez, V. García, J. Garza, W. Orellana, A. Vásquez-Espinal and W. Tiznado, $(Li_6Si_5)_{2-5}$: The Smallest Cluster-Assembled Materials based on Aromatic Si_5^{6-} Rings, *Chem.–Eur. J.*, 2019, **25**, 2467–2471.
41 O. Yañez, D. Inostroza, B. Usuga-Acevedo, A. Vásquez-Espinal, R. Pino-Rios, M. Tabilo-Sepulveda, J. Garza, J. Barroso, G. Merino and W. Tiznado, Evaluation of restricted probabilistic cellular automata on the exploration of the potential energy surface of $Be_6B_{11}^-$, *Theor. Chem. Acc.*, 2020, **139**, 41.
42 O. Yañez, R. Báez-Grez, J. Garza, S. Pan, J. Barroso, A. Vásquez-Espinal, G. Merino and W. Tiznado, Embedding a Planar Hypercoordinate Carbon Atom into a $[4n + 2]$ π-System, *ChemPhysChem*, 2020, **21**, 145–148.
43 R. Báez-Grez, J. Garza, A. Vásquez-Espinal, E. Osorio, W. A. Rabanal-León, O. Yañez and W. Tiznado, Exploring the Potential Energy Surface of Trimetallic Deltahedral Zintl Ions: Lowest-Energy $[Sn_6Ge_2Bi_6Ge_2Bi]^{3-}$ and $[(Sn_6Ge_2Bi)_2]$ Structures, *Inorg. Chem.*, 2019, **58**, 10057–10064.
44 J. M. Millam, V. Bakken, W. Chen, W. L. Hase and H. B. Schlegel, Ab initio classical trajectories on the Born–Oppenheimer surface: Hessian-based integrators using fifth-order polynomial and rational function fits, *J. Chem. Phys.*, 1999, **111**, 3800–3805.
45 M. J. Frisch, G. W. Trucks, H. B. Schlegel, G. E. Scuseria, M. A. Robb, J. R. Cheeseman, G. Scalmani, V. Barone, G. A. Petersson, H. Nakatsuji, X. Li, M. Caricato, A. V. Marenich, J. Bloino, B. G. Janesko, R. Gomperts, B. Mennucci, H. P. Hratchian, J. V. Ortiz, A. F. Izmaylov, J. L. Sonnenberg, D. Williams-Young, F. Ding, F. Lipparini, F. Egidi, J. Goings, B. Peng, A. Petrone, T. Henderson, D. Ranasinghe, V. G. Zakrzewski, J. Gao, N. Rega, G. Zheng, W. Liang, M. Hada, M. Ehara, K. Toyota, R. Fukuda, J. Hasegawa, M. Ishida, T. Nakajima, Y. Honda, O. Kitao, H. Nakai, T. Vreven,K. Throssell, J. A. Montgomery Jr, J. E. Peralta, F. Ogliaro, M. J. Bearpark, J. J. Heyd, E. N. Brothers, K. N. Kudin, V. N. Staroverov, T. A. Keith, R. Kobayashi, J. Normand, K. Raghavachari, A. P. Rendell, J. C. Burant, S. S. Iyengar, J. Tomasi, M. Cossi, J. M. Millam, M. Klene, C. Adamo, R. Cammi, J. W. Ochterski, R. L. Martin, K. Morokuma, O. Farkas, J. B. Foresman and D. J. Fox, *Gaussian 16, Revision B.01*, Gaussian, Inc., Wallingford CT, 2016.

 This journal is © The Royal Society of Chemistry 2020

Open Access Article. Published on 11 August 2020. Downloaded on 12/8/2025 10:52:22 PM.
This article is licensed under a Creative Commons Attribution-NonCommercial 3.0 Unported Licence.

46 D. Y. Zubarev and A. I. Boldyrev, Developing paradigms of chemical bonding: adaptive natural density partitioning, *Phys. Chem. Chem. Phys.*, 2008, **10**, 5207–5217.
47 D. Y. Zubarev and A. I. Boldyrev, Revealing intuitively assessable chemical bonding patterns in organic aromatic molecules *via* adaptive natural density partitioning, *J. Org. Chem.*, 2008, **73**, 9251–9258.
48 E. D. Glendening and F. Weinhold, Natural resonance theory: I. General formalism, *J. Comput. Chem.*, 1998, **19**, 593–609.
49 A. E. Reed, R. B. Weinstock and F. Weinhold, Natural population analysis, *J. Chem. Phys.*, 1985, **83**, 735–746.
50 J. P. Foster and F. Weinhold, Natural hybrid orbitals, *J. Am. Chem. Soc.*, 1980, **102**, 7211–7218.
51 E. Hückel, Quantentheoretische Beiträge zum Benzolproblem, *Zeitschrift für Phys.*, 1931, **70**, 204–286.
52 E. Hückel, Zur Quantentheorie der Doppelbindung, *Zeitschrift für Phys.*, 1930, **60**, 423–456.
53 E. Hückel, Quanstentheoretische Beiträge zum Benzolproblem, *Zeitschrift für Phys.*, 1931, **72**, 310–337.
54 J. Jusélius, D. Sundholm and J. Gauss, Calculation of current densities using gauge-including atomic orbitals, *J. Chem. Phys.*, 2004, **121**, 3952–3963.
55 D. Sundholm, H. Fliegl and R. J. F. Berger, Calculations of magnetically induced current densities: theory and applications, *Wiley Interdiscip. Rev.: Comput. Mol. Sci.*, 2016, **6**, 639–678.
56 J. Jusélius and D. Sundholm, Ab initio determination of the induced ring current in aromatic molecules, *Phys. Chem. Chem. Phys.*, 1999, **1**, 3429–3435.
57 T. A. Keith and R. F. W. Bader, Calculation of magnetic response properties using a continuous set of gauge transformations, *Chem. Phys. Lett.*, 1993, **210**, 223–231.
58 R. F. W. Bader and T. A. Keith, Properties of atoms in molecules: magnetic susceptibilities, *J. Chem. Phys.*, 1993, **99**, 3683–3693.
59 T. A. Keith and R. F. W. Bader, Topological analysis of magnetically induced molecular current distributions, *J. Chem. Phys.*, 1993, **99**, 3669–3682.
60 Y. Mo and P. v. R. Schleyer, An energetic measure of aromaticity and antiaromaticity based on the Pauling–Wheland resonance energies, *Chem.–Eur. J.*, 2006, **12**, 2009–2020.
61 Y. Mo and S. D. Peyerimhoff, Theoretical analysis of electronic delocalization, *J. Chem. Phys.*, 1998, **109**, 1687–1697.
62 J. J. Torres-Vega, A. Vásquez-Espinal, L. Ruiz, M. A. Fernández-Herrera, L. Alvarez-Thon, G. Merino and W. Tiznado, Revisiting Aromaticity and Chemical Bonding of Fluorinated Benzene Derivatives, *ChemistryOpen*, 2015, **4**, 302–307.
63 A. Vásquez-Espinal, R. Pino-Rios, L. Alvarez-Thon, W. A. Rabanal-León, J. J. Torres-Vega, R. Arratia-Perez and W. Tiznado, New Insights into $Re_3(\mu\text{-}Cl)_3Cl_6$ Aromaticity. Evidence of σ- and π-Diatropicity, *J. Phys. Chem. Lett.*, 2015, **6**, 4326–4330.
64 R. Báez-Grez, L. Ruiz, R. Pino-Rios and W. Tiznado, Which NICS method is most consistent with ring current analysis? Assessment in simple monocycles, *RSC Adv.*, 2018, **8**, 13446–13453.
65 R. Báez-Grez, D. Inostroza, V. García, A. Vásquez-Espinal, K. J. Donald and W. Tiznado, Aromatic ouroboroi: heterocycles involving a σ- donor–acceptor bond and $4n + 2\pi$-electrons, *Phys. Chem. Chem. Phys.*, 2020, **22**, 1826–1832.
66 E. D. Glendening and F. Weinhold, Natural resonance theory: II. Natural bond order and valency, *J. Comput. Chem.*, 1998, **19**, 610–627.
67 K. B. Wiberg, Application of the Pople-Santry-Segal CNDO method to the cyclopropylcarbinyl and cyclobutyl cation and to bicyclobutane, *Tetrahedron*, 1968, **24**, 1083–1096.
68 R. Peverati, P. P. Bera, T. J. Lee and M. Head-Gordon, Formation and Stability of $C_6H_3^+$ Isomers, *J. Phys. Chem. A*, 2014, **118**, 10109–10116.